Supplementary Information

A novel mesoionic carbene based highly fluorescent Pd(II) complex as an endoplasmic reticulum tracker in live cells

Sanjay K. Verma,[a] Pratibha Kumari,[b] Shagufi Naz Ansari,[a] Mohd Ovais Ansari,[a] Dondinath Deori[a] and Shaikh M. Mobin*[a,b,c]

[a]Discipline of Chemistry, [b]Discipline of Biosciences and Biomedical Engineering and [c]Discipline of Metallurgy Engineering and Materials Science, Indian Institute of Technology Indore, Simrol, Khandwa Road, Indore 453552, India

Table of Contents

Movies

Experimental Section:

Materials and general instruments:

All reactions were carried out under nitrogen atmosphere using Schlenk techniques. Glassware was oven dried at 100 °C. Solvents were distilled by standard procedures prior to use. ^{1}H NMR (400 MHz), and ^{13}C NMR (400 MHz) spectra were collected on the Bruker Avance (III) instrument by using $CDCl_3$ and DMSO-d_6. ^{1}H NMR chemical shifts are reported in parts per million (ppm) in relation to the solvent residual peak ($CDCl_3$, 7.25 ppm; DMSO-d_6, 2.49 ppm). Chemical shifts of ^{13}C NMR are presented relative to the solvent residual peak ($CDCl_3$, 77.00 ppm; DMSO-d_6, 39.50 ppm). The FTIR spectra [400−4000 cm^{-1}] were obtained with a Bio-Rad FTS 3000MX instrument on KBr pellets. UV-Visible analysis were performed on a Varian UV-vis spectrophotometer (model: Cary 100) using a quartz cuvette with a path length of 1 cm. The mass spectrum of 1 was recorded by Brucker-Daltonics, micrOTOF-QII mass spectrometer.

Synthesis of 1-methyl-4-(p-tolyl)-1H-1,2,3-triazole:

4-Ethynyltoluene (97%), (252.0 mg, 2.0 mmol) and sodium azide (130 mg, 2.0 mmol) were suspended in a 1:1 mixture of water and *tert*-butyl alcohol (10 mL). After 30 minutes CH_3I (excess) was added. Further sodium ascorbate (5.0 mol %) was added, followed by copper (II) sulfate pentahydrate (1.0 mol %). The heterogeneous mixture was stirred for 10-12 hour, progress of the reaction was continuously monitored by TLC which indicates complete consumption of the reactants (Scheme 1). The reaction mixture was diluted with water (10 mL), cooled in ice, and the white colour precipitate was collected by filtration. Precipitate was washed with cold water (2×10 mL) and dried under vacuum and further purified by column chromatography by elution of 10% ethyl acetate and hexane mixture. Yield: 320 mg (1.85 mmol, 92.4 %). ^{1}H NMR (400 MHz, DMSO-d_6) ppm δ: 8.4318 (s, 1H, Ctrz−H),

7.7136−7.6935 (d, J_{HH} = 8.04 Hz, 2H, HAr), 7.2476−7.2275 (d, J_{HH} = 8.04 Hz, 2H, HAr), 4.0637 (s, 3H, N−CH_3), 2.3131 (s, 3H, C−CH_3) ppm. ^{13}C NMR (400 MHz, DMSO-d_6) ppm δ: 146.43 (Ctrz−Ar), 137.03 (Ctrz−H), 129.40 (*C*Ar−Ctrz), 128.04 (*C*Ar−CH_3), 125.01 (*C*Ar−Ctrz), 121.81 (*C*Ar−Ctrz), 36.33 (N−*C*H_3), 20.79 (C−*C*H_3) ppm. DMF (3 mL) was added to the resulting compound (100 mg, 0.531 mmol) and CH_3I (excess). The solution was heated to 100 °C for 48 h. The reaction mixture was cooled to ambient temperature and to this was added diethyl ether (20 mL). The yellow coloured solid was filtered and washed with excess amount of diethyl ether. We have taken this compound directly for the preparation of complex1.

Synthesis of Pd(II) complex 1:

To a mixture of 1,3-dimethyl-4-(4'-methylbenzene-1,2,3-triazolium Iodide salt (157 mg, 0.5 mmol), K_2CO_3 (138 mg, 1.0 mmol), $PdCl_2$ (88 mg, 0.5 mmol) and KI (excess) was added pyridine (5 mL). The resulting suspension was stirred for 24 h at 80 °C. The pyridine was removed in *vacuo* and the crude mixture was extracted with dichloromethane (15 mL). The solvent was removed and the yellow residue was loaded onto a silica gel column. Elution with a hexane:ethyl acetate (6:4, v:v) mixture gave compound **1** as a yellow solid. Yield: 187 mg (0.298 mmol, 60 %). ^{1}H NMR (400 MHz, $CDCl_3$) ppm δ: 8.9272 (d, 2H, HPy), 7.8001−7.7825 (d, J_{HH} = 7.04 Hz, 2H, HPy), 7.6633 (m, 1H, HPy), 7.3717−7.3541 (d, J_{HH} = 7.04 Hz, 2H, HAr), 7.2500 (d, 2H, HAr), 4.4162 (s, 3H, N−CH_3), 3.9244 (s, 3H, N−CH_3), 2.4460 (s, 3H, C−CH_3) ppm. ^{13}C NMR (400 MHz, $CDCl_3$) ppm δ: 153.81 (CPy), 144.13 (Ctrz−Ar), 140.01 (CPy), 137.31 (Ctrz−Pd), 133.50 (CAr−H), 130.19 (CAr−H), 129.46 (*C*Ar−Ctrz), 124.26 (CPy), 42.97 (N−CH_3), 37.21 (N−CH_3), 21.53 (C−*C*H_3) ppm.

Quantum yield calculation:

The fluorescence quantum yield (Φ_F) of 1 was calculated using eqn (1) by the steady-state comparative method using quinine sulfate as the standard ($\Phi_{st} = 0.54$)[1]

$$\Phi_F = \Phi_{st} \times S_u/S_{st} \times A_{st}/A_u \times \eta^2_{Du}/\eta^2_{Dst} \qquad (1)$$

where Φ_F is the emission quantum yield of the sample, Φ_{st} is the emission quantum yield of the standard, S_u and S_{st} are the integrated emission band areas of the sample and the standard, respectively, while A_{st} and A_u represent the absorbance of the standard and the sample at the excitation wavelength, respectively, and n_{Du} and n_{Dst} are the solvent refractive index of the sample and the standard, and u and st refer to the unknown and the standard, respectively.

X-ray crystallography:

The crystal data of **1** was collected at 293 K by the means of graphite-monochromated Mo Kα (λα = 0.71073 Å). The strategy for the data collection was evaluated by the help of CrysAlisPro CCD software. The data were collected by the standard phi-omega scan techniques and were scaled and reduced using CrysAlisPro RED software. The structures were solved by the direct methods by using SHELXS-2014 and refined by full matrix least squares with SHELXL-2014, refining on F^2.[2] by direct methods the positions of all the atoms were obtained and all nonhydrogen atoms were refined anisotropically. All the remaining hydrogen atoms were placed in geometrically constrained positions and refined with isotropic temperature factors, generally 1.2 × Ueq of their parent atoms. The hydrogen bonding interactions, molecular drawings and mean-plane analysis were obtained using the Diamond (ver. 3.1d). [3] The crystal and refinement data are summarized in Table S1 and the selected bond distances and bond angles are shown in Table S2.

Cell viability assay[4]:

Approx. 7000 Hela (cervical cancer) cells and HEK 293 (Human embryonic kidney cells 293) normal cell line were seeded in in 96-well plate in 100 µL complete DMEM (DMEM, 10% (v/v) FBS and 1% antibiotics, Penicillin Streptomycin10,000 U/mL). Compound **1** was serial diluted in DMSO and added to media (0.1% DMSO in each well). The original media from each removed and 200 µL new media including compound (concentration ranging from 20 µM- 180 µM) added in each well. Each concentration experiment was performed in triplicate. Further cells were incubated for 24 h at 37 °C and 5% CO2 atmosphere followed by washing with phosphate buffered saline (PBS pH 7.4). 100 µL MTT (1 mg/mL in phenol red free media) was added in each well and further incubated 4 hours at 37℃. Media rinsed and 100 µL DMSO added in order to dissolve purple formazan crystals. After 15 minutes shaking, absorbance at 570 nm was measured using Synergy H1 Biotek microplate reader. The % cell viability was calculated as: % cell viability = [Mean O.D. of the drug treated cell/Mean O.D. of the control well] × 100

Per-pixel spatial colocalization analysis

A significance test was performed for the images in blue (probe **1**) and red (ER Tracker red) channels using Costes' method [5] and the P-value was found to be 1.00, which indicates that a randomized image set does not produce better correlation/colocalization than the real image. Furthermore, Manders' coefficients were calculated based on the formulae presented by Manders et al.[6]

***In vitro* photostability study**

Cervical cancer cell line HeLa was seeded in two confocal dishes. Dishes were incubated with **1** (100 µM for 8 h) and ER Tracker Red (1 µM, 30 min) separately. The cells were

imaged using confocal microscope with no delay scan mode. Videos were recorded up to 1800 for ER Tracker Red and **1** respectively. ER Tracker Red and **1** ware excited at 559 nm and 405 nm respectively. Maximum intense signal of first scan was considered 100% for measuring relative decrease in intensity. Images at every 200 scans were obtained from video.

Flow cytometry:

HeLa cells were cultured in six-well tissue culture plates. When cells became 80% confluent then one well left without treatment with probe as control and another well treated with **1** (100μM) for 8 h. followed by washing with PBS three times. Cells were harvested by trypsin/EDTA and re-suspended in PBS. The samples were analyzed by BD LSRFortessa ™ Flow cytometry with excitation at 405 nm and emission 415-470 nm. Data were analyzed by DB FACSDiva software. Total 10,000 events were acquired for each sample.

The selectivity of subcellular organelle:

Cervical cancer (HeLa) cell line was seeded in three confocal dishes and incubated for 24 h at 37°C and 5% CO_2 atmosphere. Then 100 μM **1** was added in each disc for 8 h followed by washing twice with PBS. The live cells were co-stain with ER-Tracke Red (1μM) for ER imaging, LysoTracker Red (100 nM) for lysosome imaging and MitoTracker Red (80 nM,) for mitochondria imaging. After incubation for 30 min, the live cells were washed with PBS four times. Subcellular localization analysis of **1** and ER-Tracke Red were imaged by confocal microscope. An Olympus laser scanning microscope was used for confocal imaging. **1** was excited 405 nm and emission collected at 415–470 nm**;** ER-Tracke Red, LysoTracker Red DND99 as well as MitoTracker Red CMXRos were excited at 559 nm and fluorescence was collected at 580–700 nm.

Cell imaging:

HeLa cells were grown overnight on a confocal microscope dish with a cover slip and 100 μM **1** was added to cells for 8 h. After washing twice with PBS, the live cells were stained with 500nM ER-Tracke Red for 30 min and washed with PBS three times. Subcellular localization analysis of **1** and ER-Tracke Red was imaged by confocal microscope. **1** was excited 405 nm and emission collected at 415–470 nm**;** ER-Tracker Red was excited at 559 nm and fluorescence was collected at 580–700 nm.

Generation of multicellular 3D spheroids:

Multicellular tumor spheroids (MCTSs) were produced using the liquid overlay method.[7] when HeLa cells became 60% confluent in T-25 flack, they were harvested by trypsin/EDTA solution and resuspended in Dulbecco's Modified Eagle's Medium (DMEM) complete media. Flat-bottom 96 well plates were coated with 80μL of a sterile 1.5% (wt/vol) agarose solution in complete DMEM to make a non-adherent surface. 600 cells were seeded in each agarose-coated well in 150μl complete DMEM. The plates were incubated at 37°C and 5% CO_2 until spheroids formed. Spheroid were transfers in confocal disc followed by spheroids treatment by 100μM **1** for 8 h, then image captured by confocal laser scanning microscopy.

Table S1 Crystal data and structure refinement for **1.**

Identification code	**1**
CCDC	1573135
Empirical formula	$C_{16}H_{18}I_2N_4Pd$
Formula weight	626.54
Temperature/K	293(2)
Crystal system	monoclinic
Space group	$P2_1/n$
a/Å	10.7786(5)
b/Å	8.1520(3)
c/Å	23.4486(10)
α/°	90
β/°	99.338(4)
γ/°	90
Volume/Å^3	2033.06(15)
Z	4
ρ_{calc}g/cm^3	2.047
μ/mm^{-1}	3.953
F(000)	1176.0
Crystal size/mm^3	0.25 × 0.23 × 0.2
Radiation	MoKα (λ = 0.71073)
2Θ range for data collection/°	6 to 57.682
Index ranges	$-14 \le h \le 13$, $-10 \le k \le 11$, $-29 \le l \le 31$
Reflections collected	11043
Independent reflections	4670 [R_{int} = 0.0283, R_{sigma} = 0.0267]
Data/restraints/parameters	4670/0/211
Goodness-of-fit on F^2	1.045
Final R indexes [I>=2σ (I)]	R_1 = 0.0434, wR_2 = 0.1117
Final R indexes [all data]	R_1 = 0.0488, wR_2 = 0.1154
Largest diff. peak/hole / e Å^{-3}	1.80/-1.33

Table S2 Bond Lengths and Bond Angles for **1.**

Bond Length/Å		Bond Angles/°	
Pd1− I2	2.5935(5)	I2 −Pd1 −I1	176.52(2)
Pd1− I1	2.6107(5)	N4 −Pd1 −I2	90.46(12)
Pd1− N4	2.100(4)	N4 −Pd1 −I1	91.59(12)
Pd1− C9	1.968(5)	C9 −Pd1 −I2	87.89(14)
N3 −N2	1.337(6)	C9 −Pd1 −I1	90.13(14)
N3 −C9	1.363(6)	C9 −Pd1 −N4	177.77(17)
N3 −C11	1.464(7)	N2 −N3 −C9	114.2(4)
N1 −C8	1.368(6)	N2 −N3 C−11	117.8(4)
N1 −N2	1.319(6)	C9 −N3 −C11	128.0(4)
N1 −C10	1.470(7)	C8 −N1 −C10	129.8(5)
C8 −C5	1.473(7)	N2 −N1 −C8	112.7(4)
C8 −C9	1.387(7)	N2 −N1 −C10	117.4(4)
N4 −C12	1.325(8)	N1 −C8 −C5	123.4(4)
N4−C16	1.327(7)	N1 −C8 −C9	106.3(4)
C5− C4	1.388(7)	C9 −C8 −C5	130.3(4)
C5 − C6	1.384(8)	C12 −N4 −Pd1	122.5(4)
C4 −C3	1.377(8)	C12 −N4 −C16	116.5(5)
C6 −C7	1.393(9)	C16 −N4 −Pd1	121.0(4)
C7 −C2	1.394(10)	N1 −N2 −N3	103.5(4)
C2 −C3	1.368(10)	C4 −C5 −C8	121.2(5)
C2 −C1	1.501(9)	C6 −C5 −C8	119.9(5)
C13 −C12	1.383(9)	C6 −C5− C4	118.9(5)
C13 −C14	1.349(10)	C3 −C4 −C5	120.4(6)
C14 −C15	1.349(10)	C5 −C6 −C7	119.7(6)
C16 −C15	1.376(9)	N3 −C9 −Pd1	124.5(4)
		N3 −C9 −C8	103.4(4)
		C8 −C9 −Pd1	132.1(3)
		C6 −C7 −C2	121.2(6)
		C7 −C2 −C1	121.2(7)
		C3 −C2 −C7	117.9(6)
		C3 −C2 −C1	120.9(7)
		C2 −C3 −C4	121.7(6)
		C14 −C13 −C12	119.6(7)
		N4 −C12 −C13	122.8(6)
		C13 −C14 −C15	118.4(6)
		N4 −C16 −C15	123.2(6)
		C14 −C15 −C16	119.5(6)

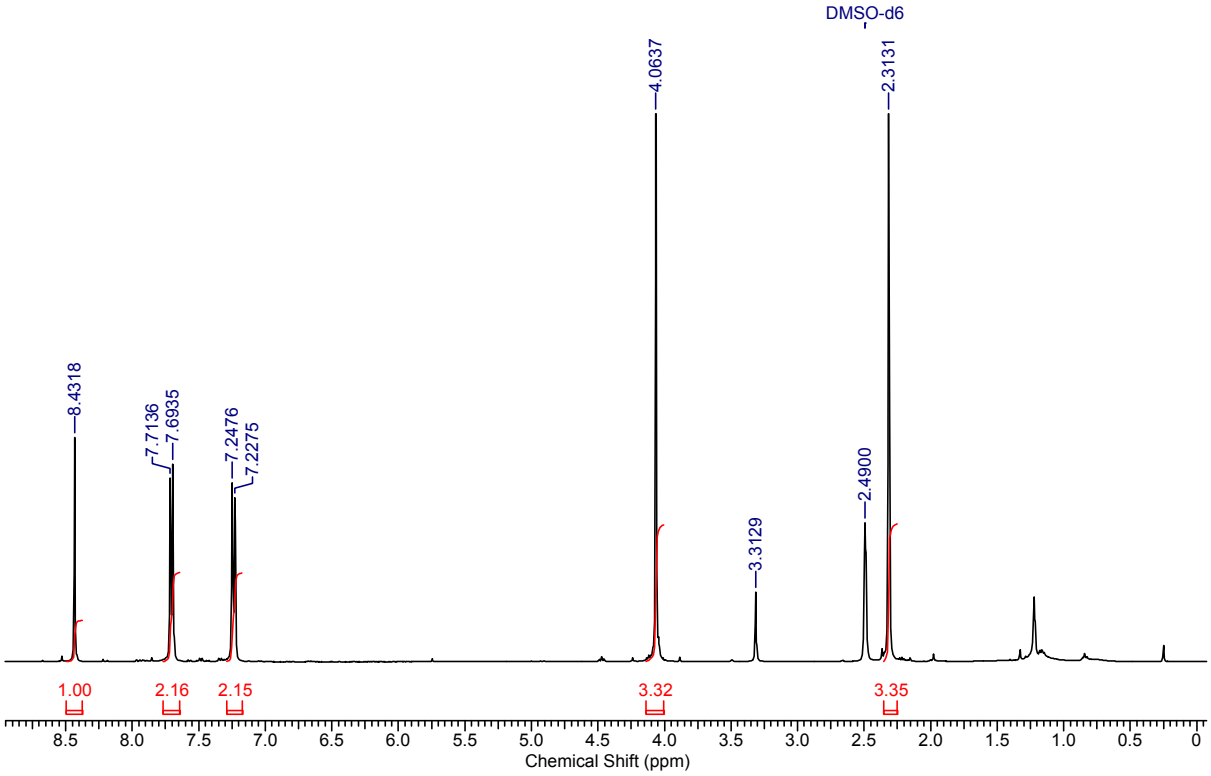

Fig. S1 [1]H NMR Spectrum of 1-methyl-4-(p-tolyl)-1H-1,2,3-triazole. (DMSO-d6)

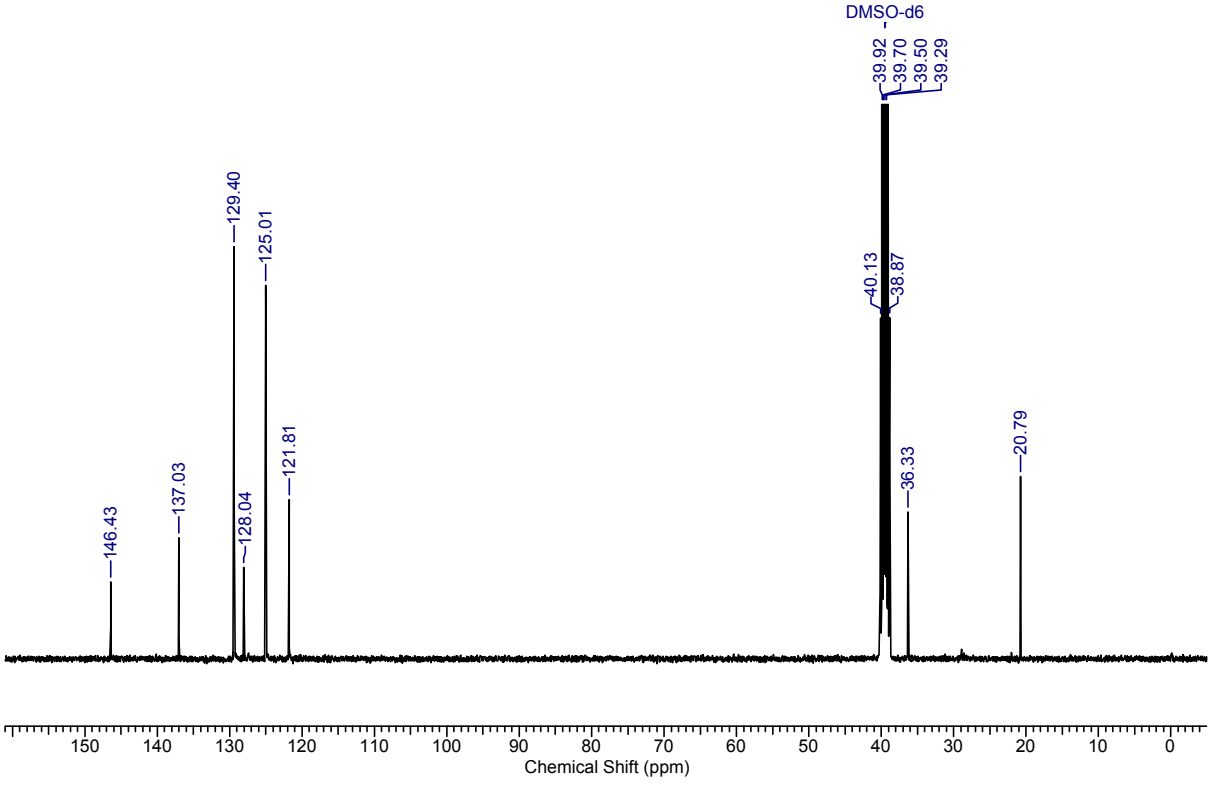

Fig. S2 [13]C NMR Spectrum of 1-methyl-4-(p-tolyl)-1H-1,2,3-triazole (DMSO-d_6).

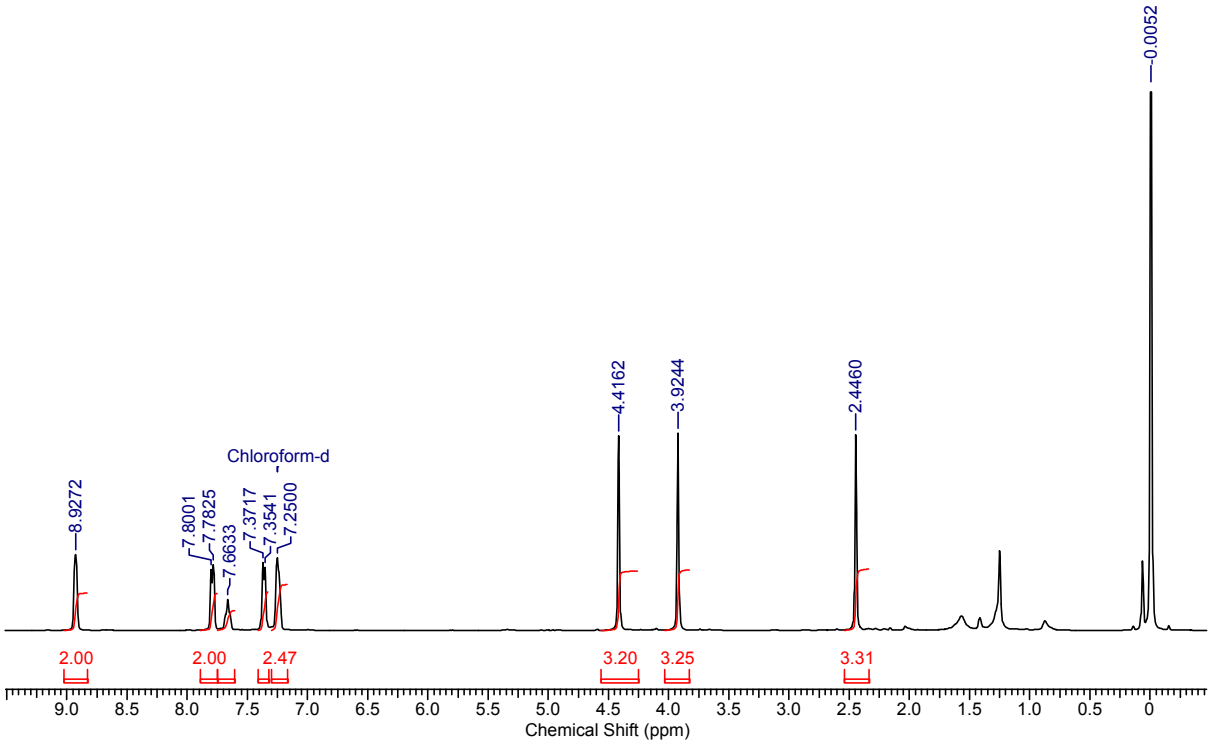

Fig. S3 ^{1}H NMR Spectrum of **1.**

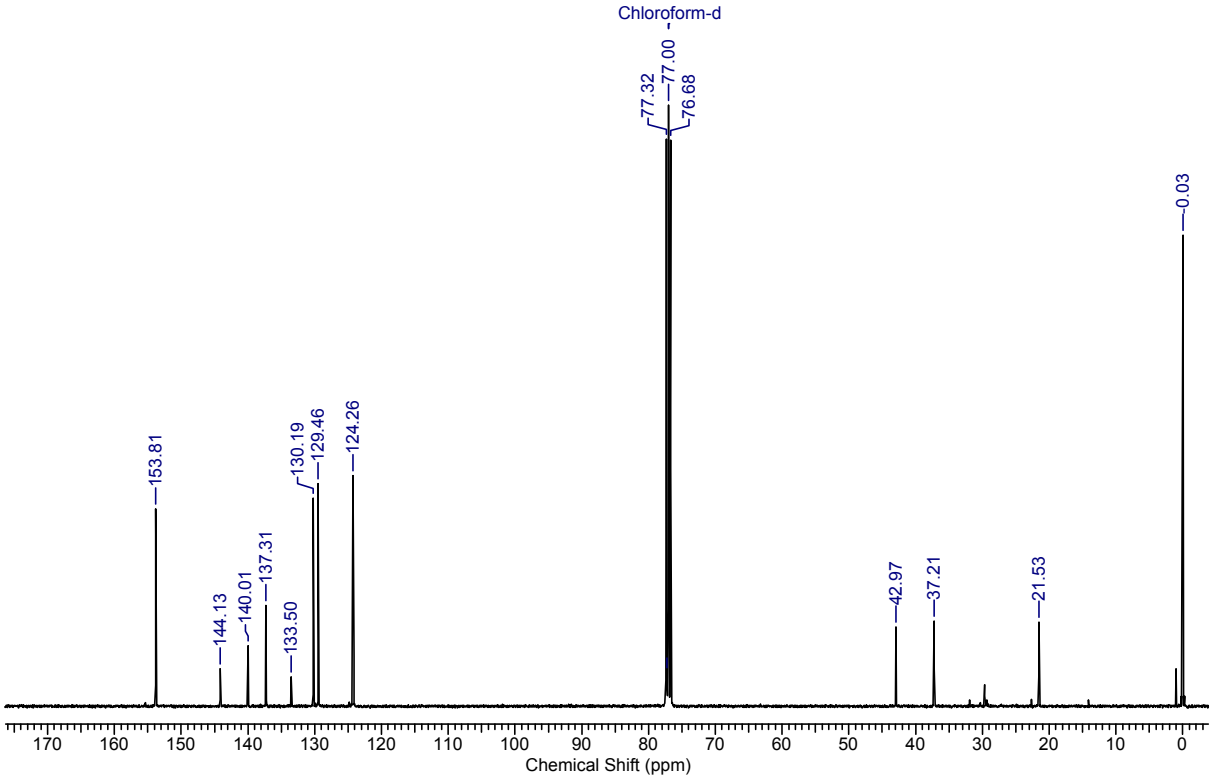

Fig. S4 ^{13}C NMR Spectrum of **1.**

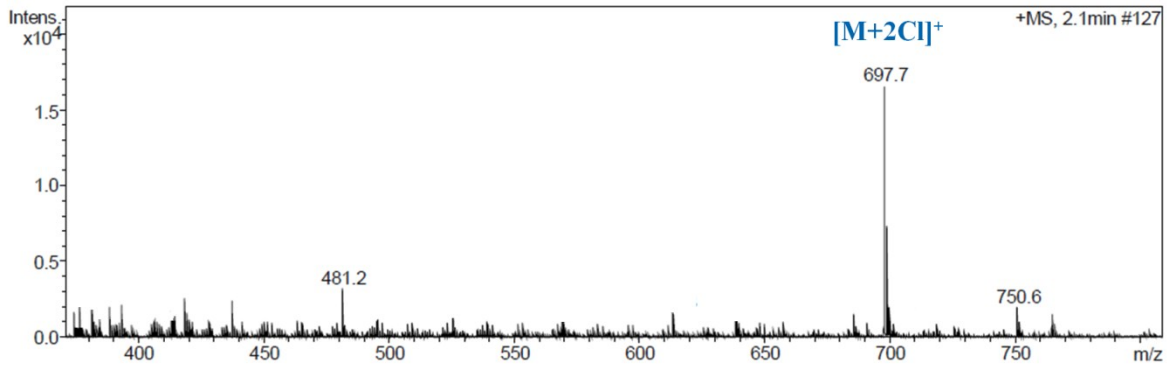

Fig. S5 LC-MS spectrum of the complex **1**.

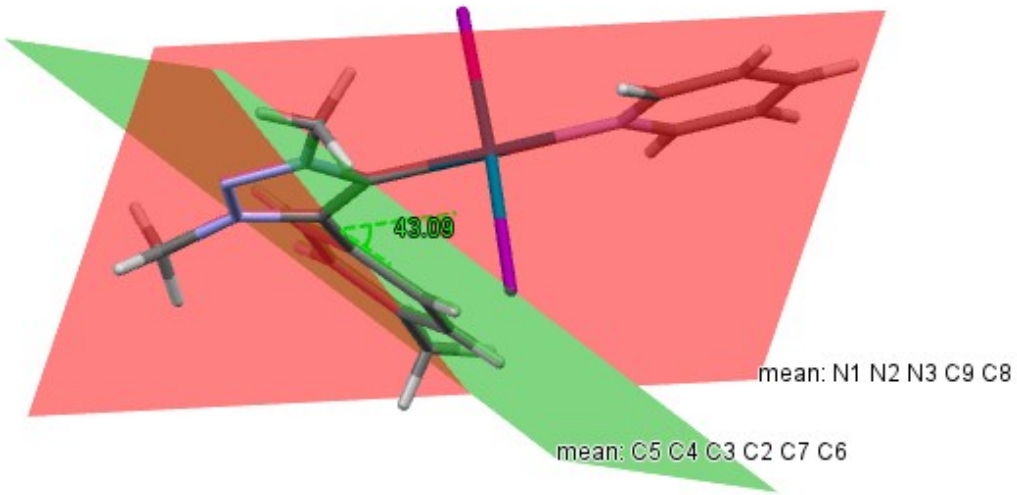

Fig. S6 Dihedral angle between the NHC plane {N1 N2 N3 C8 C9} and the phenyl ring plane {C2 C3 C4 C5 C6 C7} is measured to be 43.09°.

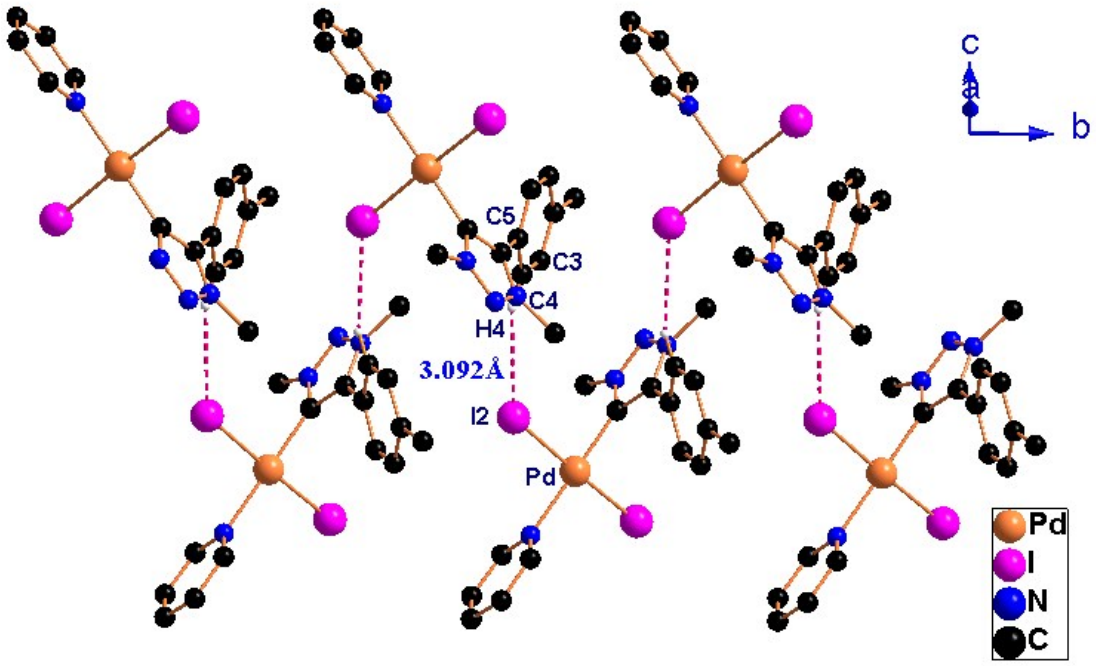

Fig. S7 Supramolecular architecture of **1** via I2...H4−C4 alog b-axis.

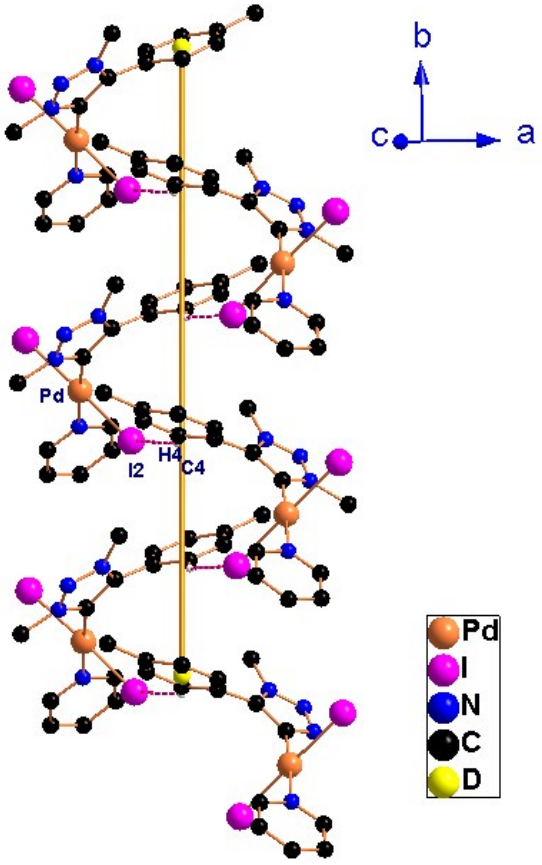

Fig. S8 Formation of single strainded helical structure of **1** via I2...H4−C4 alog b-axis.

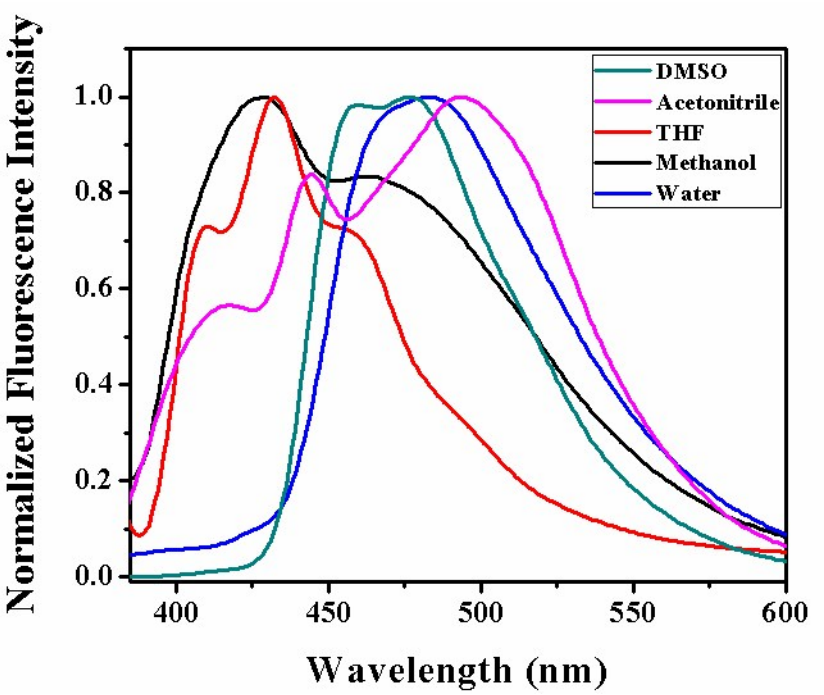

Fig. S9 Emission spectrum of Pd(II) complex **1** in 1.0% DMSO and some other solvents (DMSO/Acetonitrile/THF/Methanol/Water) upon excitation at 371 nm.

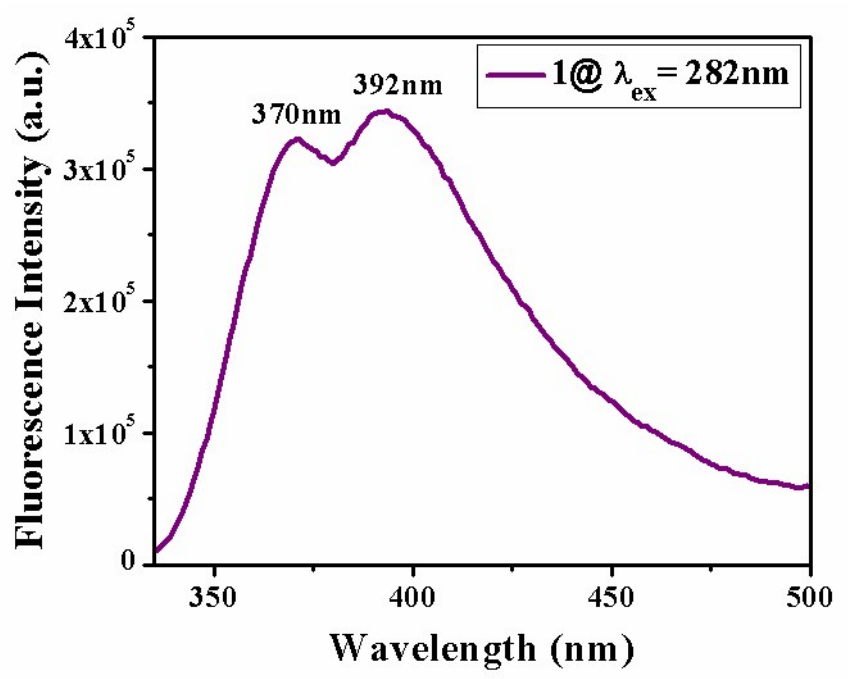

Fig. S10 Photoluminescence spectrum of the complex **1** at room temperature in solid state.

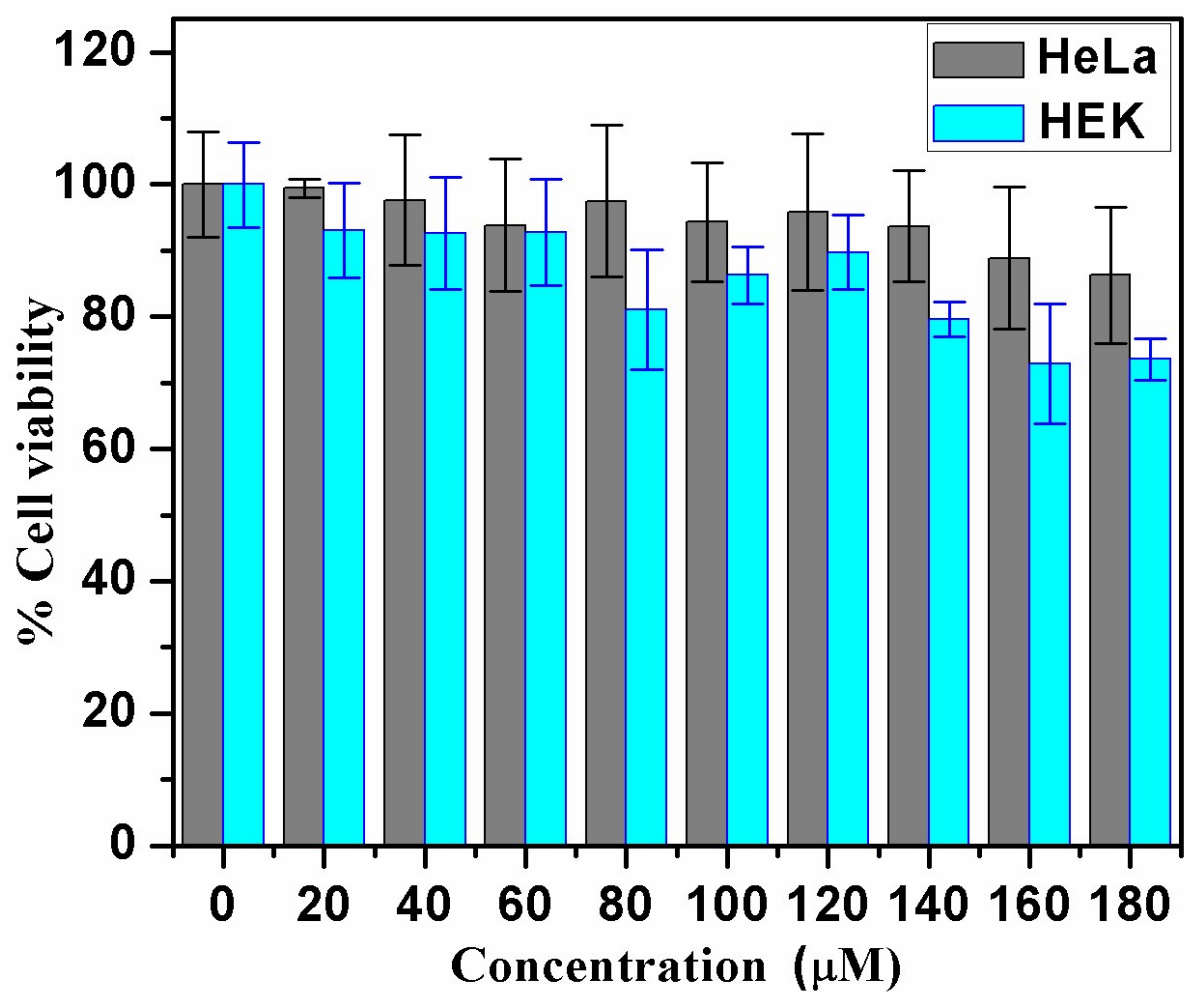

Fig. S11 Cell viability study of probe **1** on HeLa (cervical cancer cells) and HEK 293 (Human embryonic kidney cells 293) normal cells by the MTT assay after 24 h incubation at 37°C and the results shown in mean ± SD of three separate measurements.

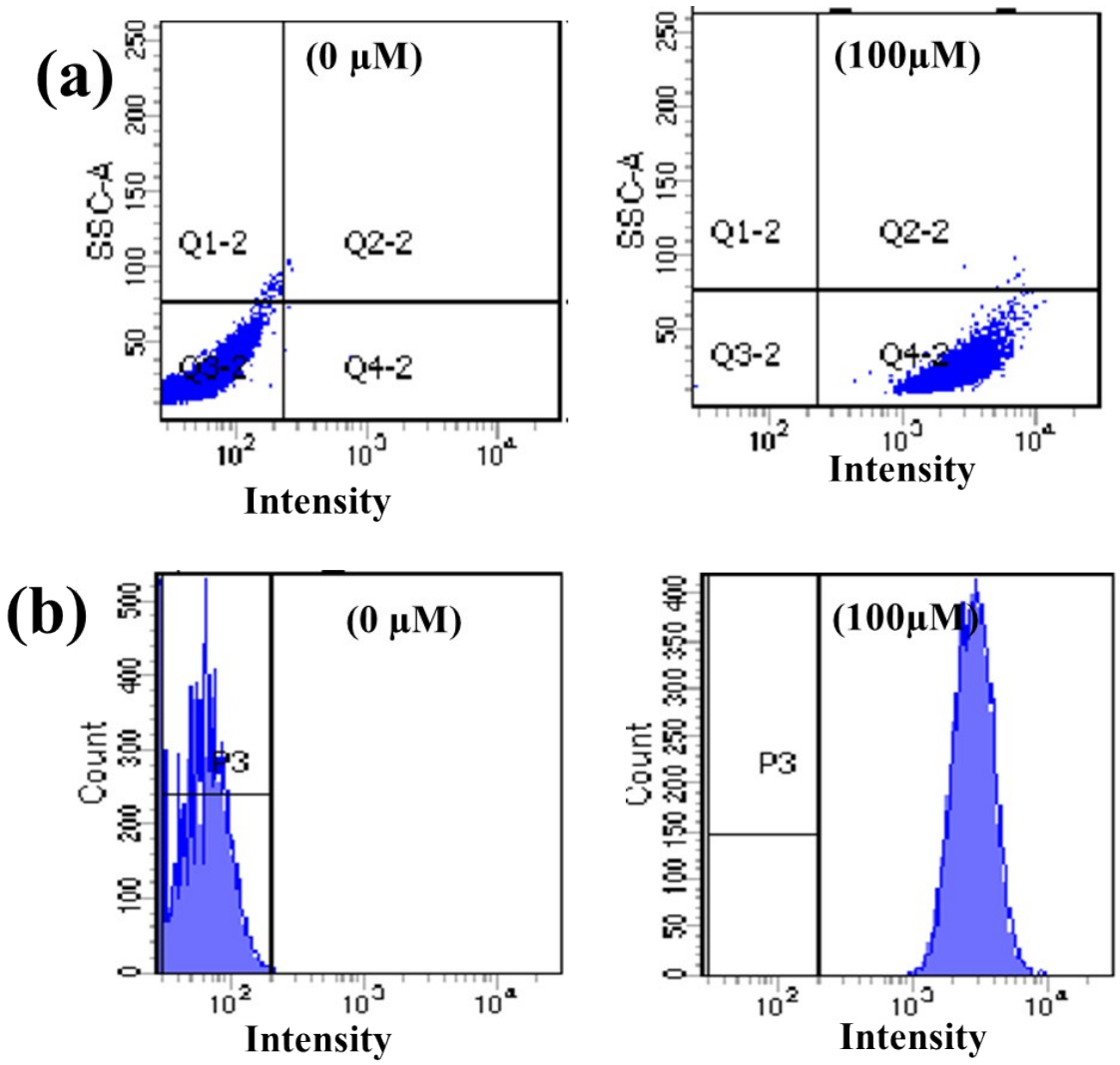

Fig. S12 Flow cytometric analysis of probe **1** label large population of Living HeLa cells in suspension: (**a**) Scatter plot. (**b**) Histogram. **1**, λ_{ex} = 405 nm; λ_{em} = 415-470 nm.

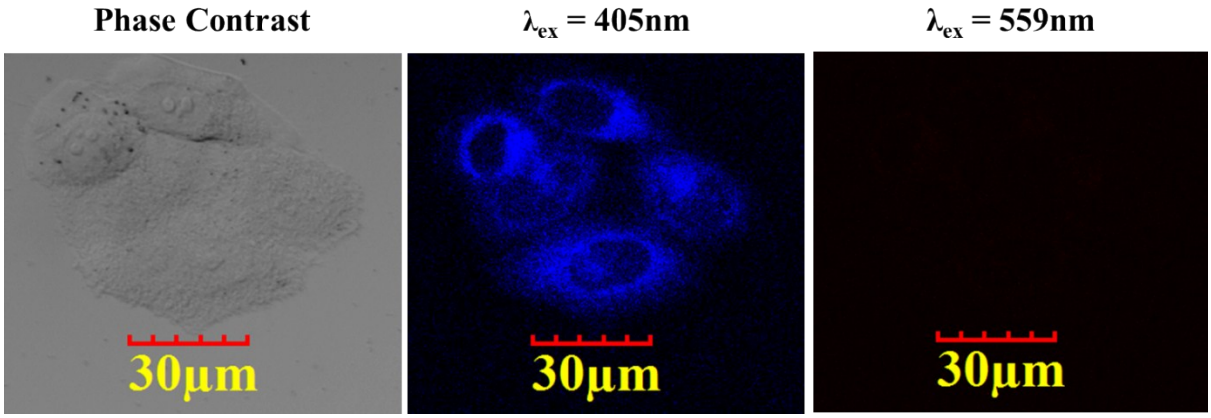

Fig. S13 HeLa cells were treated with probe **1** and image where captured in blue and red channels. λ_{ex} =405nm; λ_{em} = 415-470 nm; λ_{ex} = 559 nm; λ_{em} = 580-700 nm.

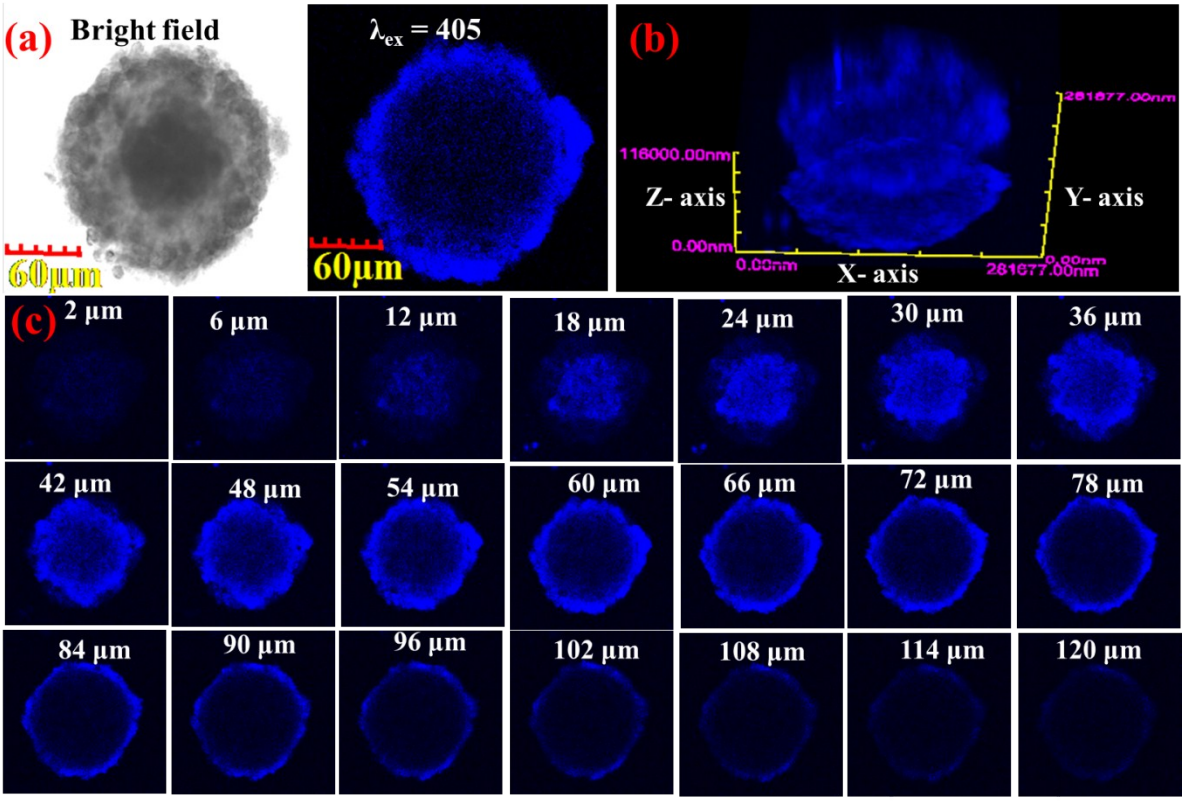

Fig. S14 (a) Fluorescence images of 3D intact HeLa tumor spheroid after incubation of **1**(100 µM) for 8 h) by confocal laser scanning microscope. (b) The Z-stack 3D images of intact spheroid. (c) The Z-stack images were captured after every 2 µm section from the top to bottom of tumor spheroid. The images were taken under a 10× objective λex = 405 nm; λem = 415–470 nm.

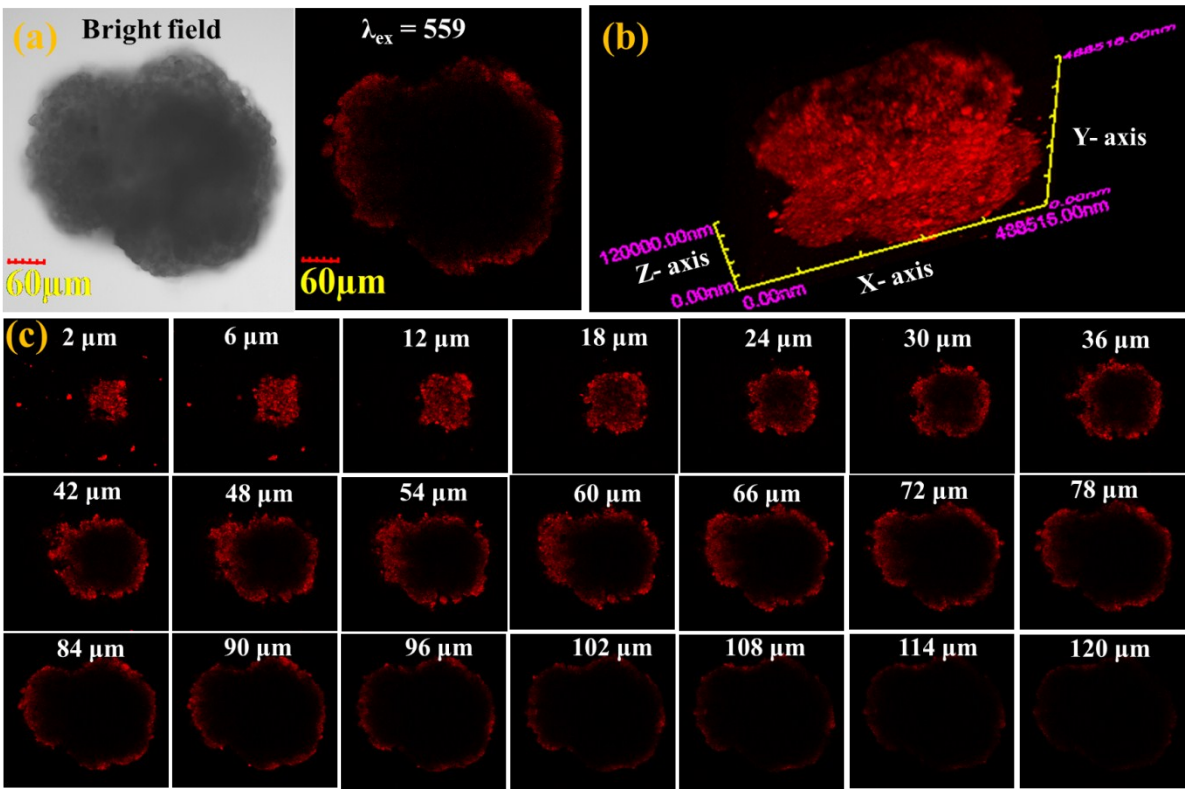

Fig. S15 (a) Fluorescence images of 3D intact HeLa tumor spheroid after incubation of ER tracker (1.0 μM) for 8 h) by confocal laser scanning microscope. (b) The Z-stack 3D images of intact spheroid. (c) The Z-stack images were captured after every 2 μm section from the top to bottom of tumor spheroid. The images were taken under a 20× objective λex = 559 nm; λem = 569–600 nm.

Movies

Movie S1. Photostability of **1** on HeLa cells by confocal microscopy.

Movie S2. Photostability of ER tracker Red on HeLa cells by confocal microscopy.

Movie S3. Fluorescence of 3D intact tumor spheroid after incubation of **1.** The Z-stack images were captured after every 2 μm section from the top to bottom of tumor spheroid.

Movie S4. Fluorescence of 3D intact tumor spheroid after incubation of ER tracker. The Z-stack images were captured after every 2 μm section from the top to bottom of tumor spheroid.

References:

1. A. K. Saini, M. Srivastava, V. Sharma, V. Mishra and S. M. Mobin, *Dalton Trans.*, 2016, **45**, 3927.
2. G. M. Sheldrick, Acta Cryst., 2015, **C71**, 3.
3. Scientific Computing World. 2002, **63**, 19.
4. A. K. Saini, V. Sharma, P. Mathur and M. M. Shaikh, *Sci. Rep.* 2016, **6**, 34807.
5. S. V. Costes, D. Daelemans, E. H. Cho, Z. Dobbin, G. Pavlakis and S. Lockett, *Biophys J.* 2004, **86**, 3993.
6. E. M. M. Manders, F.J. Verbeek, J. A. Aten, *J. Microsc*. 2004, **169**, 375
7. J. Friedrich, C. Seidel, R. Ebner, L. A. Kunz-Schughart, *Nat. Protoc.* 2009, **4**, 309.